

Wall-wake laws for the mean velocity and the turbulence

Alexander J. Smits

Department of Mechanical and Aerospace Engineering, Princeton University,
Princeton, NJ, USA

(6 February 2024)

A new wall-wake law is proposed for the streamwise turbulence in the outer region of a turbulent boundary layer. The formulation pairs the logarithmic part of the profile (with a slope A_1 and additive constant B_1) to an outer linear part, and it accurately describes over 95% of the boundary layer profile at high Reynolds numbers. Once the slope A_1 is fixed, B_1 is the only free parameter determining the fit. Most importantly, B_1 is shown to be proportional to the wake factor in the wall-wake law for the mean velocity, revealing a previously unsuspected connection between the turbulence and the mean flow.

1. Introduction

The mean velocity distribution in the outer part of a turbulent boundary layer is often expressed as a combination of a logarithmic part and a wake component, as in

$$\frac{U}{u_\tau} = \frac{1}{\kappa} \ln \frac{yu_\tau}{\nu} + B + \frac{2\Pi}{\kappa} W\left(\frac{y}{\delta}\right), \quad (1.1)$$

where U is the mean velocity in the streamwise direction, $u_\tau = \sqrt{\tau_w/\rho}$, τ_w is the shear stress at the wall where $y = 0$, ρ is the fluid density, κ is von Kármán's constant, B is the additive constant, and Π is the Reynolds number dependent wake factor. The wake function W is taken to be a universal function of y/δ , where δ is the outer layer length scale. This wall-wake model was first formulated by Coles (1956), and it is an essential part of the widely-used composite profile derived by Chauhan *et al.* (2007).

Marusic *et al.* (1997) proposed a similar formulation for the streamwise turbulence intensity in zero pressure gradient turbulent boundary layers, given by

$$\overline{u^2}^+ = B_1 - A_1 \ln \frac{y}{\delta_m} - V_g \left(y^+, \frac{y}{\delta_m} \right) - W_g \left(\frac{y}{\delta_m} \right), \quad (1.2)$$

where $\overline{u^2}^+ = \overline{u^2}/u_\tau^2$. The model incorporates the log-law for $\overline{u^2}^+$ with constants A_1 and B_1 (Hultmark *et al.* 2012; Marusic *et al.* 2013), where V_g is a mixed scale viscous deviation term, W_g is the wake deviation term, and δ_m is a boundary layer thickness defined in a way that is similar to the Rotta-Clauser thickness. It is typically 15 to 20% larger than δ_{99} , the 99% thickness (further details are given in the Appendix). The wake deviation was given by

$$W_g = B_1 \eta^2 (3 - 2\eta) - A_1 \eta^2 (1 - \eta)(1 - 2\eta), \quad (1.3)$$

where $\eta = y/\delta_m$.

Pirozzoli & Smits (2023) recently proposed an alternative model for the mean velocity distribution in the outer layer, given by a compound logarithmic-parabolic distribution

of the type first suggested by Hama (1954). That is,

$$\frac{U_e - U}{u_\tau} = B - \frac{1}{k_0} \ln \frac{y}{\delta_0}, \quad (1.4)$$

$$\frac{U_e - U}{u_\tau} = C \left(1 - \frac{y}{\delta_0}\right)^2, \quad (1.5)$$

where C is a constant, and U_e is the freestream velocity. Requiring the two velocity distributions to smoothly connect up to the first derivative yields the position of the matching point ($\eta_0 = y_0/\delta_0$) and the additive constant B in (1.4) as a function of k_0 and C ,

$$\eta_0 = \frac{1}{2} \left(1 - \left(1 - \frac{2}{Ck_0}\right)^{1/2}\right), \quad B = C(1 - \eta_0)^2 + \frac{1}{k_0} \log \eta_0. \quad (1.6)$$

In what they called the classical case, Pirozzoli & Smits (2023) found that with $\delta_0 = 1.6\delta_{95}$ the best fit of the data was obtained with $k_0 = \kappa \approx 0.38$, $C \approx 9.88$, so that $B = 2.15$, with the two distributions smoothly matched at $\eta_0 = 0.158$. This compound logarithmic-parabolic distribution fits the velocity distributions well down to $y/\delta_0 \approx 0.01$ (for Reynolds numbers based on displacement thickness greater than 2000).

Here, we suggest a similar approach for the streamwise component of the turbulent stress. That is, we propose a compound representation given by

$$\overline{u^2}^+ = B_1 - A_1 \ln \frac{y}{\delta_1}, \quad (1.7)$$

$$\overline{u^2}^+ = b_1 - a_1 \frac{y}{\delta_1}, \quad (1.8)$$

where a_1 , and b_1 are constants, and δ_1 is the appropriate length scale for the outer layer. In this formulation, there is no viscous deviation term. Requiring the two turbulence distributions to smoothly connect up to the first derivative yields the position of the matching point ($\eta_1 = y_1/\delta_1$) and the additive constant B_1 in (1.7) as a function of the other constants,

$$\eta_1 = \frac{A_1}{a_1}, \quad B_1 = b_1 - A_1(1 - \ln \eta_1). \quad (1.9)$$

According to (1.8), $\overline{u^2}^+$ is zero when $y/\delta_1 = b_1/a_1$, and so we impose one further constraint and set $b_1/a_1 = 1.05$ (which closely corresponds to the point where $y/\delta_{99.5} = 1$). Finally, if we assume A_1 is a true constant ($= 1.26$ for boundary layers according to Marusic *et al.* (2013)), the only free parameter in our fit to the turbulence profile is B_1 , which we will show to be Reynolds number dependent and proportional to the mean velocity wake factor Π .

2. Comparisons with data

We now demonstrate the quality of the model by comparing it with experimental and DNS data over a wide range of Reynolds numbers (see table 1). Before proceeding, we need to specify the particular length scale δ_1 used to describe the outer layer. We have chosen $\delta_1 = \delta_{99}$, for reasons made clear in the Appendix. We also need to relate $Re_\theta = \theta U_e/\nu$, where θ is the momentum thickness, to the friction Reynolds number $Re_\tau = \delta_{99} u_\tau/\nu$, in that not all data sets specify both. This issue is also addressed in the Appendix.

To begin the analysis, we use the data by Samie *et al.* (2018) ($6250 < Re_\theta < 47,100$).

	Re_θ	Re_τ	b_1	B_1	η_1	Symbol
DeGraaff & Eaton (2000)	1430	541	3.56	1.05	0.372	●
	2900	993	3.77	1.19	0.351	■
	5200	1692	4.33	1.57	0.306	▲
	13000	4336	4.83	1.94	0.274	◆
	31000	10023	4.67	1.82	0.276	○
Fernholz <i>et al.</i> (1995)	2573	866	4.10	1.42	0.323	●
	5023	1692	4.34	1.59	0.305	■
	7140	2375	4.80	1.92	0.276	▲
	16080	5068	5.30	2.29	0.250	◆
	20920	6824	4.75	1.88	0.279	○
	41300	12633	4.75	1.88	0.279	□
	57720	18692	4.95	2.03	0.267	△
	60810	18362	4.95	2.03	0.267	◇
Osaka <i>et al.</i> (1998)	6040	1800	4.75	1.88	0.279	●
Vallikivi <i>et al.</i> (2015)	8402	2622	4.90	1.99	0.270	●
	15121	4635	5.00	2.07	0.265	■
	26884	8261	4.85	1.95	0.273	▲
	46732	14717	4.80	1.92	0.276	◆
	80579	25062	3.82	1.22	0.346	○
	133040	40053	3.57	1.06	0.371	□
	234670	68392	3.23	0.845	0.410	△
Samie <i>et al.</i> (2018)	6252	1929	4.92	2.00	0.269	●
	12913	3984	4.96	2.04	0.267	■
	26034	8032	5.10	2.14	0.259	▲
	47096	14530	4.88	1.98	0.271	◆
Sillero <i>et al.</i> (2013)	6000	1848	4.530	1.72	0.292	- - - -

TABLE 1. Data sources and fitting parameters for $A_1 = 1.96$. B_1 is the only free parameter, and b_1 and the matching point η_1 are defined by (1.9).

Figure 1 demonstrates that, as expected from previous work, the log part with $A_1 = 1.26$ and $B_1 = 2.00$ is a good fit in the overlap region. In addition, the linear part of the model describes the profile beyond the matching point very well over this range of Reynolds numbers, except for the region $y/\delta_{99} > 1$ where a more gradual decline is observed. At the highest Reynolds numbers, the compound formulation represents the data well for 95% of the profile.

For reference, we also plot (1.2) for the same values of A_1 and B_1 (using $\delta_{99}/\delta_m = 0.81$). We neglected the viscous deviation term V_g , which leads to a positive offset of (1.2) with respect to the compound in the logarithmic region. Both fits work well beyond the logarithmic region, although it could be argued that the linear fit is a trifle more accurate for $0.2 < y/\delta_{99} < 0.9$. In our analysis going forward, we will use compound fit, primarily because the viscous deviation term in (1.2) appears to obscure some of the underlying trends as well as the comparisons between the turbulence and mean velocity profiles.

We now consider all the high Reynolds number data listed in table 1 over the range $6000 \leq Re_\theta < 60,000$ (the Vallikivi *et al.* profiles for $Re_\theta > 60,000$ will be dealt with separately). The results are shown in figure 2 for $B_1 = 2.00$. Although there is some the scatter in the data, the compound fit works reasonably well using this value. The

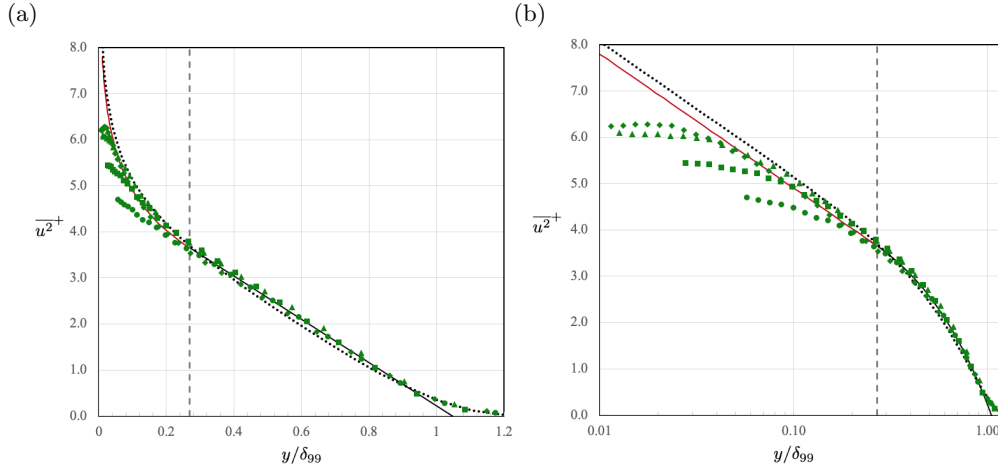


FIGURE 1. Comparison to the experimental data of Samie *et al.* (2018) for $Re_\theta = 6252\text{--}47096$ ($y^+ > 100$, $A_1 = 1.26$, $B_1 = 2.00$). (a) Linear scaling. (b) Log scaling. $\cdots\cdots$, (1.2) (neglecting V_g); --- , (1.7); --- , (1.8) (matched at $\eta_1 = 0.269$, vertical dashed line). Symbols as in table 1.

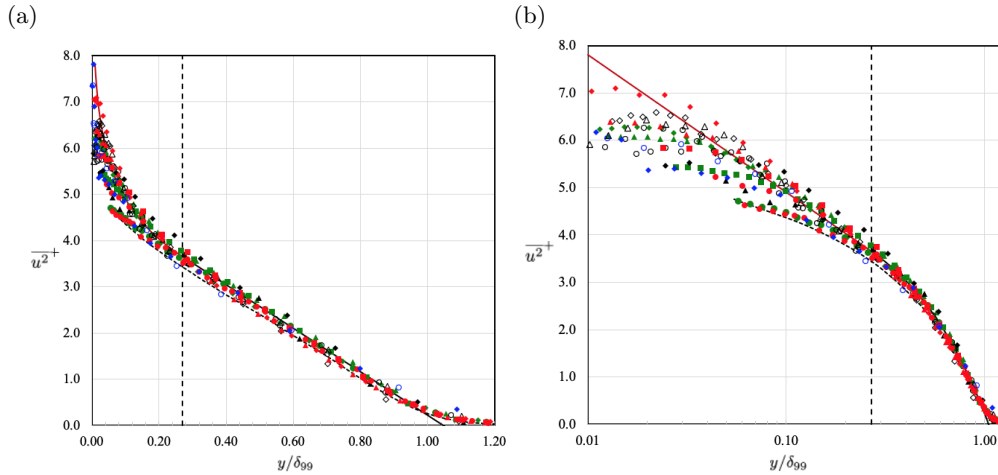


FIGURE 2. Comparison to all the experimental data for $6000 \leq Re_\theta < 60,000$ ($y^+ > 100$). Symbols as in table 1. (a) Linear scaling. (b) Log scaling. --- , (1.8); --- , (1.7). $B_1 = 2.00$, distributions matched at $\eta_1 = 0.269$ (vertical dashed line).

agreement can be improved by using values of B_1 optimized for each profile, as listed in table 1.

The low Reynolds number data ($Re_\theta \leq 6040$) are shown in figure 3. The compound fit is plotted for two cases, $B_1 = 2.00$ (the value used for the high Reynolds number data shown in figures 1 and 2), and $B_1 = 1.05$ (chosen to match the lowest Reynolds number profile in the data set). In order to match the in-between Reynolds number cases, B_1 was varied as given in table 1. Again, we see a very satisfactory fit to the data, even in this low Reynolds number range.

We now consider the highest Reynolds number data, where $Re_\theta > 60,000$. There are only three profiles available, at $Re_\theta = 80,579$, $133,040$, and $234,670$ (Vallikivi *et al.* 2015). They are unique, in the sense that no other turbulence data exist at comparable Reynolds

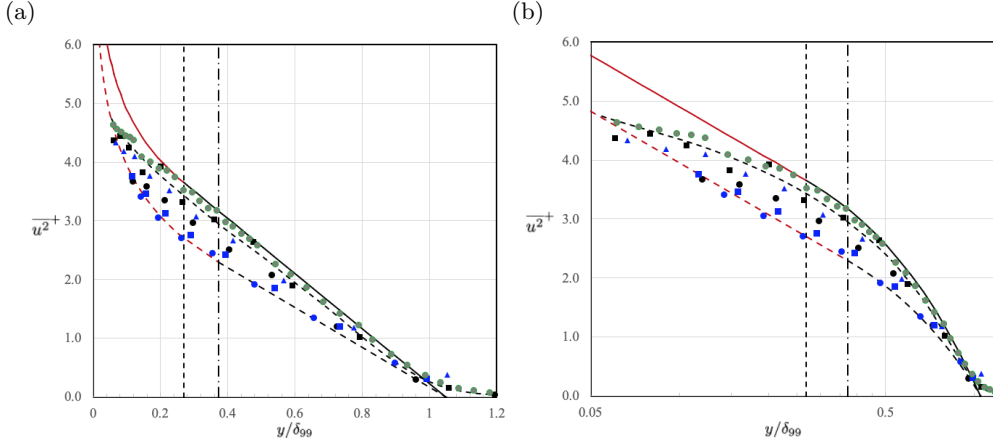


FIGURE 3. Comparison to the experimental data for $Re_\theta \leq 6040$ ($y^+ > 100$). Symbols as in table 1. (a) Linear scaling. (b) Log scaling. —, (1.8); —, (1.7). $b_1 = 4.92$, distributions matched at $\eta_1 = 0.269$ (vertical dashed line). - - - -, (1.8); - - - -, (1.7). $b_1 = 3.56$, distributions matched at $\eta_1 = 0.372$ (vertical dashed-dotted line).

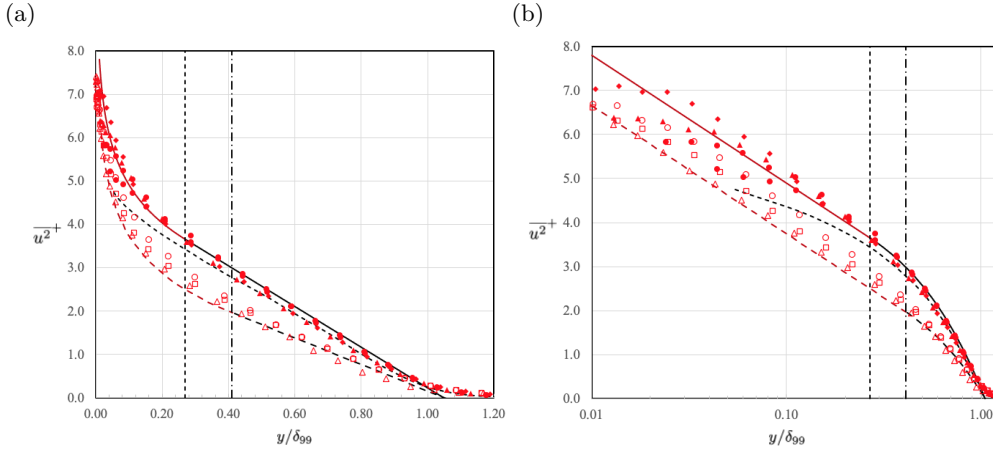


FIGURE 4. Comparison to the experimental data for $Re_\theta > 60,000$ ($y^+ > 100$). Symbols as in table 1. (a) Linear scaling. (b) Log scaling. —, (1.8); —, (1.7). $b_1 = 4.92$, distributions matched at $\eta_1 = 0.269$ (vertical dashed line). - - - -, (1.8); - - - -, (1.7). $b_1 = 3.23$, distributions matched at $\eta_1 = 0.410$ (vertical dashed-dotted line).

numbers. The compound fit is shown in figure 4. Somewhat surprisingly, B_1 begins to decrease in a systematic way below its ‘high’ Reynolds number value of 2.00 (see table 1). This result may indicate a problem with the data, but it may also reflect the apparent connection between B_1 and Π .

The constant B_1 acts as a wake function for the turbulence profile, similar to the wake function Π for the mean velocity profile. In figure 5, we compare the Reynolds number dependence of B_1 with that of $2\Pi/\kappa$ (using $\kappa = 0.384$; B_1 was scaled by an arbitrary factor of 1.15 to aid the comparison). We see a clear similarity between the two wake functions for $Re_\theta < 60,000$, and they appear to be proportional to each other by a constant factor.

For $Re_\theta > 60,000$, the B_1 values decrease with Reynolds number, as noted above. However, they still tend to follow the behavior of the corresponding Π values. Although

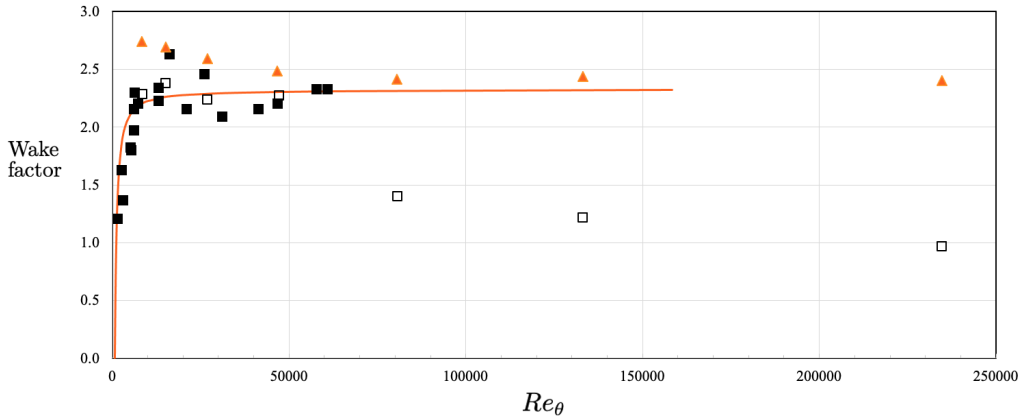


FIGURE 5. Wake factors versus Re_θ . \blacksquare , $1.15B_1$ (Vallikivi *et al.* 2015 values shown as \square); --- , $2\Pi/\kappa$ (Chauhan *et al.* 2007); \blacktriangle , $2\Pi/\kappa$ (Vallikivi *et al.* 2015).

the Π values at lower Reynolds numbers for the Vallikivi data set lie above the Chauhan correlation (which is similar to the Coles (1956) distribution, not shown here), they consistently decrease with Reynolds number before becoming approximately constant, which is also the trend followed by B_1 . This observation is not conclusive, but it helps to reinforce the notion that the two wake functions are linked.

3. Conclusions and discussion

The log-linear compound fit in y/δ_{99} proposed here for the streamwise turbulent stress $\overline{u^2}^+$ in the outer layer of a turbulent boundary layer works well over a wide range of Reynolds numbers. For the log part of the fit we assumed that A_1 , the slope of the log-law, is fixed at 1.26 (as given by Marusic *et al.* (2013)), and the linear part of the fit was constrained to pass through zero at $y/\delta_{99} = 1.05$. As a consequence, the fit has only one free parameter, B_1 , which acts like a wake factor.

For low Reynolds numbers ($Re_\theta \leq 6040$), B_1 increases with increasing Reynolds number, attaining an approximately constant value of about 2 for higher Reynolds numbers ($6000 \leq Re_\theta \leq 60,000$). At very high Reynolds numbers ($Re_\theta > 60,000$), B_1 begins to decrease with increasing Reynolds number, although this observation is based on very limited data.

The behavior of B_1 closely follows the variation of the mean flow wake factor Π , suggesting that the mean flow and the turbulence in the outer layer may be linked by a common mechanism related to the structure of turbulence. This link is clear for the log-part of the formulation, in that the mean velocity and the turbulence distributions are connected through the attached eddy hypothesis (Perry & Chong 1982; Marusic & Monty 2019). For the parabolic part of the mean velocity (1.5) and the linear part of the turbulence (1.8), the link is still unknown. One possibility is to consider the behavior of the “detached” (or Type B) eddies (Perry & Marusic 1995). However, as they note, building this connection “would be very complicated and would depend on the assumed shape of the representative eddies.” Also, as Hu *et al.* (2020) point out, “Unlike the attached eddies, whose statistical behaviours are well described by the (attached eddy hypothesis), the detached eddies lack a good phenomenological model.” In their statistically-based interpretation, the major contributions to the streamwise turbulence stress for $y/\delta > 0.25$ are equally divided between the detached eddies and the Kolmogorov-scale eddies. Un-

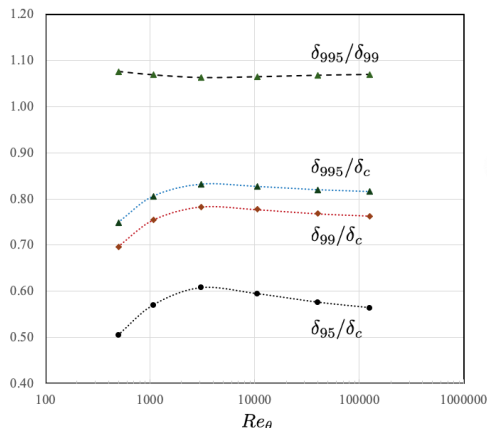


FIGURE 6. Boundary layer thickness variations with Re_θ , as found using the composite profile (Chauhan *et al.* 2007).

Understanding the physics that connects the mean velocity and the turbulence in the outer layer is clearly in need of further work.

Acknowledgements

The authors would like to thank Sergio Pirozzoli and Jean-Paul Dussauge for their comments on an earlier draft.

Declaration of interests. The author reports no conflict of interest.

Appendix: Data analysis

For the length scale used to describe the outer layer, δ_1 , there are a multitude of choices. In examining the mean flow, Pirozzoli & Smits (2023) considered $\delta_0 = 1.6\delta_{95}$, 0.28Δ (where $\Delta = (U_e/u_\tau)\delta^*$ is the Rotta-Clauser thickness), and $\delta_N = (H/(H-1))\delta^*$. For the data in table 1, Sillero *et al.* (2013), DeGraaff & Eaton (2000) and Vallikivi *et al.* (2015) used δ_{99} , Osaka *et al.* (1998) used δ_{995} , and Samie *et al.* (2018) used δ_c , where δ_c is the outer length scale adopted by Chauhan *et al.* (2007) for their composite profile. In order to compare data, we need a common standard, and we will show that $\delta_1 = \delta_{99}$ serves that purpose well. To convert δ_{995} and δ_c to the matching value of δ_{99} , we used the composite profile. In figure 6, we show how these various thicknesses compare.

We used the results of Klebanoff (1955) on the eddy viscosity. His boundary layer thickness was about 1.15 times larger than δ_{99} (Smits 2024), and the data were scaled accordingly.

In addition, we need to relate Re_θ and Re_τ , in that not all data sets specify both. Here, we use

$$Re_\theta = 3.241Re_\tau, \quad (3.1)$$

based on a fit to the available data ($R^2 = 0.9997$ for full data set). See figure 7.

Finally, the $Re_\theta = 234670$ profile by Vallikivi *et al.* (2015) was corrected for an error in the 99% thickness, which was smaller by a factor of 0.943 than the value originally reported. This changed the profile, and the corresponding value of Re_τ . Also, the Fernholz profile at $Re_\theta = 21410$ was not used since it has some obvious problems.

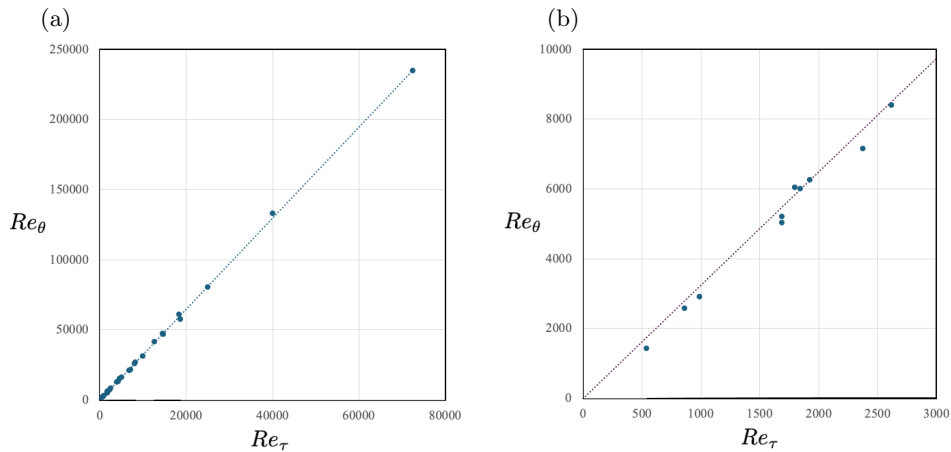


FIGURE 7. Momentum thickness Reynolds number versus friction Reynolds number. Dashed line, (3.1). (a) Full data set; (b) data for $Re_\theta < 10000$.

REFERENCES

- CHAUHAN, K., NAGIB, H. & MONKEWITZ, P. 2007 On the composite logarithmic profile in zero pressure gradient turbulent boundary layers. *AIAA Paper 2007-0532* .
- COLES, D. E. 1956 The law of the wake in the turbulent boundary layer. *J. Fluid Mech.* **1**, 191–226.
- DEGRAAFF, D. B. & EATON, J. K. 2000 Reynolds-number scaling of the flat-plate turbulent boundary layer. *J. Fluid Mech.* **422**, 319–346.
- FERNHOLZ, H.H., KRAUSE, E., NOCKEMANN, N. & SCHOBER, M. 1995 Comparative measurements in the canonical boundary layer at $Re_{\delta_2} \leq 6 \times 10^4$ on the wall of the German-Dutch windtunnel. *Phys. Fluids* **7**, 1275–1281.
- HAMA, F. R. 1954 Boundary layer characteristics for smooth and rough surfaces. *Trans. Soc. Naval Archit. Mar. Engrs.* **62**, 333–358.
- HU, R., YANG, X. I. A. & ZHENG, X. 2020 Wall-attached and wall-detached eddies in wall-bounded turbulent flows. *J. Fluid Mech.* **885**, A30.
- HULTMARK, M., VALLIKIVI, M., BAILEY, S. C. C. & SMITS, A. J. 2012 Turbulent pipe flow at extreme Reynolds numbers. *Phys. Rev. Lett.* **108** (9), 1–5.
- KLEBANOFF, P. S. 1955 Characteristics of turbulence in a boundary layer with zero pressure gradient. *NACA Report 1247* .
- MARUSIC, I. & MONTY, J. P. 2019 Attached eddy model of wall turbulence. *Annu. Rev. Fluid Mech.* **51**, 49–74.
- MARUSIC, I., MONTY, J. P., HULTMARK, M. & SMITS, A. J. 2013 On the logarithmic region in wall turbulence. *J. Fluid Mech.* **716**, R3.
- MARUSIC, I., UDDIN, M. & PERRY, A. E. 1997 Similarity law for the streamwise turbulence intensity in zero-pressure-gradient turbulent boundary layers. *Phys. Fluids* **12**, 3718–3726.
- OSAKA, H., KAMEDA, T. & MOCHIZUKI, S. 1998 Re-examination of the Reynolds-number-effect on the mean flow quantities in a smooth wall turbulent boundary layer. *JSME Int. J., Ser. B* **41** (1), 123–129.
- PERRY, A. E. & CHONG, M. S. 1982 On the mechanism of wall turbulence. *J. Fluid Mech.* **119**, 173–217.
- PERRY, A. E. & MARUSIC, I. 1995 A wall-wake model for the turbulence structure of boundary layers. Part 1. Extension of the attached eddy hypothesis. *J. Fluid Mech.* **298**, 361–388.
- PIROZZOLI, S. & SMITS, A. J. 2023 Outer-layer universality of the mean velocity profile in turbulent wall-bounded flows. *Phys. Rev. Fluids* **8** (6), 064607.
- SAMIE, M., MARUSIC, I., HUTCHINS, N., FU, M. K., FAN, Y., HULTMARK, M. & SMITS, A. J. 2018 Fully resolved measurements of turbulent boundary layer flows up to $Re_\tau = 20,000$. *J. Fluid Mech.* **851**, 391–415.

- SILLERO, J. A., JIMÉNEZ, J. & MOSER, R. D. 2013 One-point statistics for turbulent wall-bounded flows at Reynolds numbers up to $\delta^+ \approx 2000$. *Phys. Fluids* **25** (10).
- SMITS, A. J. 2024 Assessing Klebanoff's data. *Under review* .
- VALLIKIVI, M., HULTMARK, M. & SMITS, A. J. 2015 Turbulent boundary layer statistics at very high Reynolds number. *J. Fluid Mech.* **779**, 371–389.